

# A Laboratorial Prototype of a Weight Measuring System Using Fibre Bragg Gratings Embedded in Silicone Rubber

J. C. VIEIRA, A. C. VIEIRA, C. M. FRIAS, C. M. A. VASQUES  
and R. DE OLIVEIRA

## ABSTRACT

A silicone rubber tray with embedded optical fibre sensors is produced in this work. Two fibre Bragg grating (FBG) sensors are embedded in silicone rubber to enhance their sensitivity. When the rubber tray is subjected to transversal load the wavelength shift of the FBG sensors increases thanks to the coupling with the low stiffness host material. The linear dependence of the Bragg wavelength shift was measured to be 7.64 nm/Pa. A good response of the FBG sensor is observed when embedded in silicone; the sensibility to the applied load was found to be 0.0033 nm/g. This paper reports the first results on the development of a prototype of a weight measuring system using fibre Bragg gratings embedded in a silicone rubber tray.

## INTRODUCTION

Over the last two decades fibre Bragg grating (FBG) sensors were extensively studied as strain sensors for several applications. Due to the brittleness of glass optical fibres the embedment of FBG in different materials revealed to be an interesting solution, not only as an adequate protection, but, also, to safe monitoring structures where reliability is a fundamental requirement. Nowadays, they can be used in several applications in civil, aerospace and biomedical engineering areas, to name only a few. Some studies about the influence of the embedding processing methods and how different materials achieve different FBG sensibility can be found in [1-9]. The same concepts can be used in optical sensing applications involving softer materials. One of the main characteristics of soft materials is their ability to be easily deformed. They permit the development of flexible sensors, through the embedment of FBG sensors, which can be used in applications where such characteristics are required, such as clothes for biomechanical applications (to measure strain in muscles and tendons), without introducing a significant local reinforcement.

In this paper a laboratorial prototype of a weight measuring system using optical FBG sensors embedded in silicone rubber is presented. When compared to standard

---

J. C. Vieira, A. C. Vieira, C. M. Frias, C. M. A. Vasques and R. de Oliveira, INEGI, University of Porto, Campus da FEUP, Rua Dr. Roberto Frias 400, 4200-465 Porto, Portugal. E-mail: cvasques@inegi.up.pt.



scale-weights, the use of FBG sensors in this measuring system confers higher portability and electromagnetic fields immunity to the device. Another positive aspect of this system is that by measuring the deformation of the silicon tray, when submitted to a certain load, it measures weight indirectly. As a flexible system, it is less affected by surrounding instabilities. According to the selected silicone, the range of working temperatures is an issue because the calibration parameters depend on the silicone stiffness, which on its turn depends upon temperature.

### Strain Sensing using Fibre Bragg Sensors

Fibre Bragg Grating sensors, usually designated as FBG sensors, are formed when a periodic variation is recorded on the refractive index core of a photosensitive optical fibre by exposition to an ultraviolet light (UV) pattern interference [9]. When the output of a broadband light source is coupled into such an optical fibre and interacts with the grating, only a small part of the light spectrum is back reflected (Figure 1).

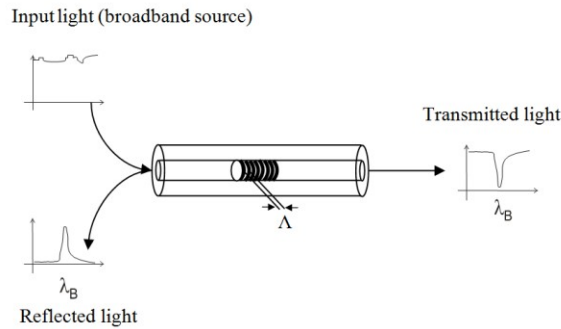


Figure 1. FBG sensor concept.

## MATERIALS AND METHODS

### Prototype Production and Calibration

For the prototype manufacturing, a mould with a 5 mm thickness and rectangular shape was made by stereolithography. The corners were cut vertically 4 mm to introduce two crossed optical fibres in the mould. A small membrane was added between the junctions of the two fibres. The mould was fulfilled with silicone rubber (SILASTIC<sup>®</sup> T-4 base with SILASTIC<sup>®</sup> T-4 O cure agent). The silicone cured during 24 hours, at room temperature, and the mould was removed. A piece of plywood with dimensions 100×100×10 mm was cut and a centred hole with 50 mm of diameter was introduced with the intent of stabilizing and supporting the silicone structure. The two pieces were attached with four board nails and can be seen in Figure 2.

Other two prototypes were made; one where the FBG's positions were changed and another one where both the silicone, changed to 10% diluted silicone rubber, and the FBG's position were changed (Figure 3).

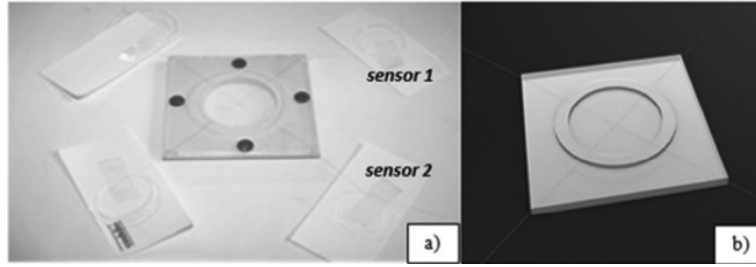


Figure 2. Laboratorial prototype of a weight measuring system: (a) photograph and (b) 3D drawing.

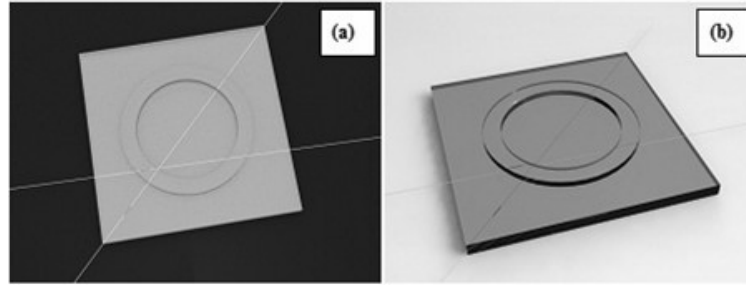


Figure 3. Prototype one (FBG placed in the diagonal and the other in vertical): (a) with silicone rubber; (b) with 10% diluted silicone rubber.

A transversal load was applied using calibrated weights (0.5g to 500g). The Bragg wavelength shift was measured using an Optical Spectrum Analyser (OSA) from Fibersensing company. The responses of both sensors were recorded simultaneously. Two different masses (5g and 15g) were used to determine the resolution of this scale weight prototype. Measures were repeated ten times and the OSA signal was registered during 30 seconds. A simple test was done to determinate the influence of the temperature in the weight measurements. This consisted in submerging the silicone rubber prototype in a reservoir with hot water and to register the signal of the FBG sensors in the OSA for five different temperatures during the cooling.

### Silicone Rubber Characterization

A Dynamic Mechanical and Thermal Analysis (DMTA) test was made to determine the admissible range of working temperatures for the two types of silicone. The test specimens were made with the following dimensions:  $16.1 \times 4.1 \times 3.3$  mm for the silicone rubber specimen and  $13.6 \times 4.04 \times 2.8$  mm for the 10% diluted silicone rubber. DMTA tensile tests were performed in a TA Instruments - DMA Q800 machine, at strain amplitude of 4% and frequency of 1Hz. The chamber temperature was risen from environment temperature until  $250^{\circ}\text{C}$ , at a heating rate of  $2^{\circ}\text{C}/\text{min}$ .

Specimens of each type of silicone rubber (see dimensions in Figure 4) were also tensile tested according to ASTM D638–03 in a universal mechanical testing machine (INSTRON 4205) to characterize the mechanical behaviour of the materials; this information was used to define the input material data necessary to the development of a representative finite element model and simulation. The tests were performed with a displacement rate of 250 mm/min with a distance between grips of 50 mm.

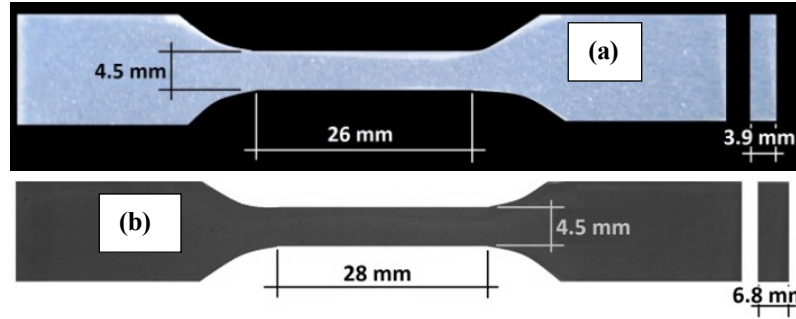


Figure 4. Test specimen made with: (a) silicone rubber and (b) 10% diluted silicone rubber.

### 3D Finite Element Modelling

A 3D finite element model of the weight prototype with a mesh of 4457 standard linear tetragonal elements was constructed in ABAQUS. An experimentally determined value of 0.9187 MPa was used to define the Young modulus of the material and a load of 20 N was applied. The model was fixed on the bottom edge sides and the load was applied in the inner circle of the upper face (see Figure 5).

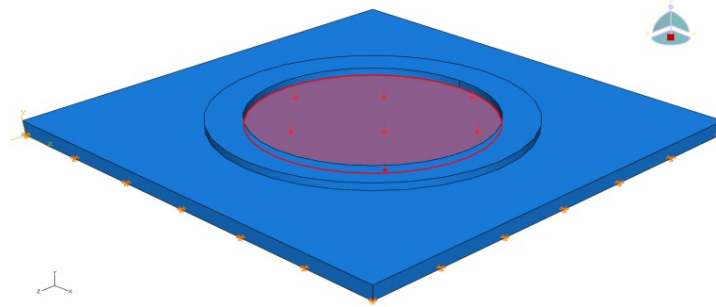


Figure 5. Scheme of boundary conditions and load.

The simulations to inquire the maximum load capacity of the prototype were performed considering the limitation of 0.4% strain of the FBG sensors. Numerical strain results in x-direction were averaged from the strain at 18 nodes around the central position.

## RESULTS AND DISCUSSION

### Prototype Calibration

As predicted, the two sensors positioned in the centre of the diagonal have the same calibration factor (around 0.003; see Figure 6a). The sensor positioned in the centre of the vertical has experienced smaller strain, since it is not aligned with the maximum strain direction (see Figure 6b). One can see in Figure 6 that in both cases the calibration points can be fitted by a linear equation.

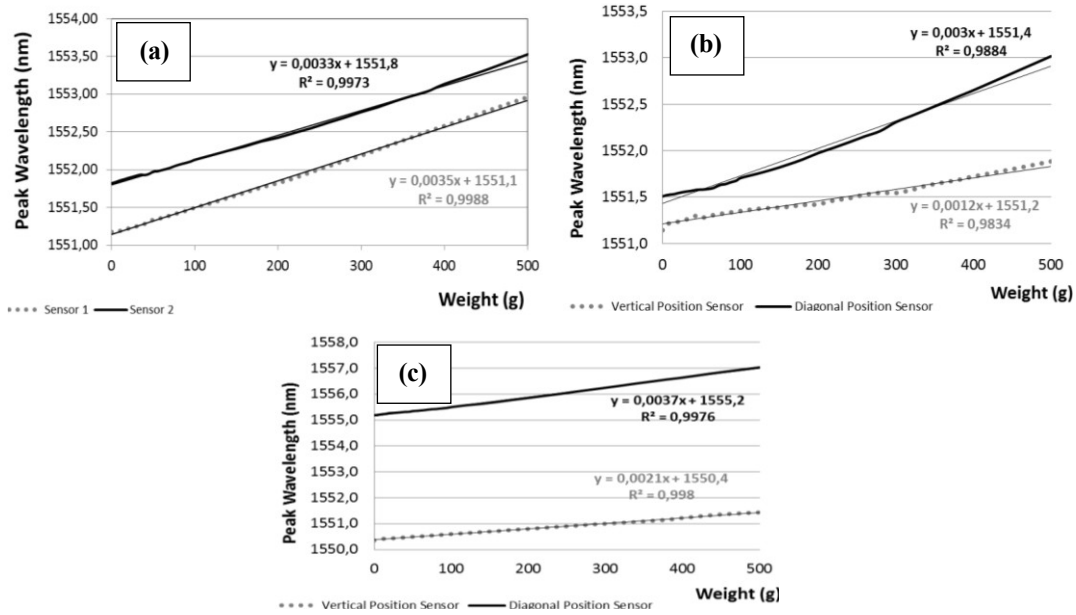


Figure 6. Prototype calibration with FBG sensors placed at different locations: (a) cross position with silicone rubber; (b) one placed in the diagonal and the other in vertical with silicone rubber; (c) one placed in the diagonal and the other in vertical with 10% diluted silicone rubber.

As expected, the 10% diluted silicone rubber showed lower stiffness compared to the prototype with normal silicone rubber (see Figures 6b and 6c). Also, this system is sensitive to temperature (see Figure 7) and therefore the calibration factor, due to the fact that both fibre and silicone expand-contract but also due to the variation of stiffness (see Figure 8), will depend upon temperature. Using two sensors it is possible to eliminate the influence of temperature since both sensors are at the same temperature.

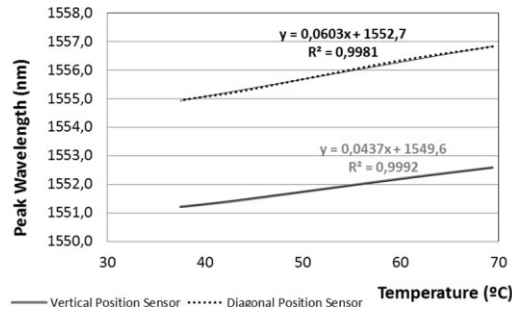


Figure 7. Variation of the central peak wavelength with temperature.

## Silicone Rubber Characterization: DMTA & Tensile Test Results

The storage and loss modulus were determined at varying temperature (see Figure 8). While the silicone T-4 steadily increased the storage modulus until 200°C (from 2 MPa to 3 MPa), the 10% diluted silicone presents a stage of nearly constant storage modulus, from environmental temperature to 100 °C, of around 0.8 MPa. Above this temperature, it will increase to 1.5 MPa at 200 °C.

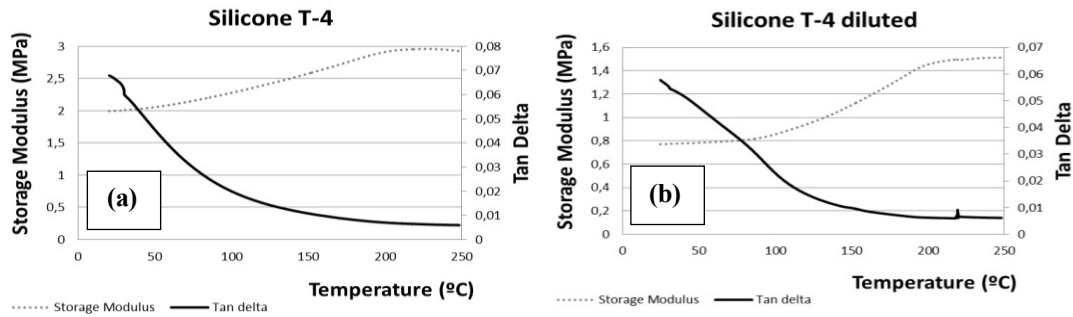


Figure 8. DMTA results for: (a) silicone rubber; (b) 10% diluted silicone rubber.

These results agree well with the tensile tests results where the 10% of dilution of the silicone rubber induces a significant decrease (roughly 50%) of the mechanical properties. The mechanical properties determined from the curves presented in Figure 9 are listed in Table 1. The Young modulus was calculated in the initial part of the stress/strain curve, by linear fitting test results up to 100% of the strain.

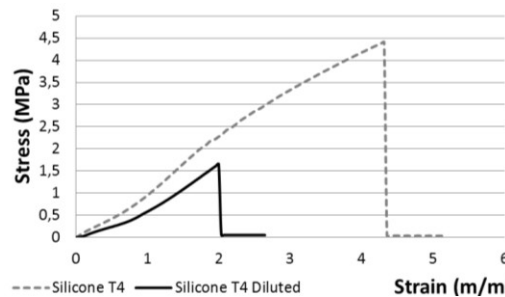


Figure 9. Tensile testing results for the two types of silicone rubber.

Table 1. Mechanical properties of the two types of silicone rubber.

	Silicone Rubber T-4	Silicone Rubber T-4 Diluted 10%
Strength (MPa)	4.406	1.653
Young modulus (MPa)	0.9187	0.5721
Strain at failure (%)	432	200

## Prototype Resolution

From Figure 10 it may be inferred that the prototype with FBG sensors placed in a cross position with silicone rubber has a good resolution (1.69 g); the signal speed response is very fast (about 0.3 s), which allows fast acquisition rates being used with good response sensitivity. This test was repeated 10 times and the results were quantitatively and qualitatively similar. This latter aspects are very important to characterize the weighing machine and results are shown for the prototype with FBG sensors placed in a cross position with silicone rubber, similar values being obtained for the other types of prototype.

## Numerical Results

As can be seen in Figure 11, the strain value for the same load is higher in the centre than parallel to the centre. This simulation verifies the experimental results, where the sensor placed in the centre is more sensible to load than the other placed parallel to the centre.



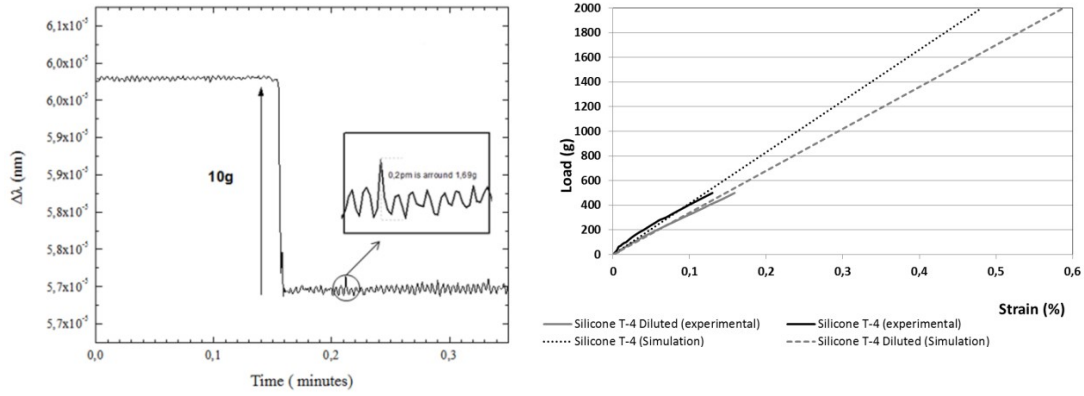


Figure 10. Prototype resolution with FBG sensors placed in a cross position with silicone rubber (left); Numerical and experimental results of the scale weight prototypes calibration (right).

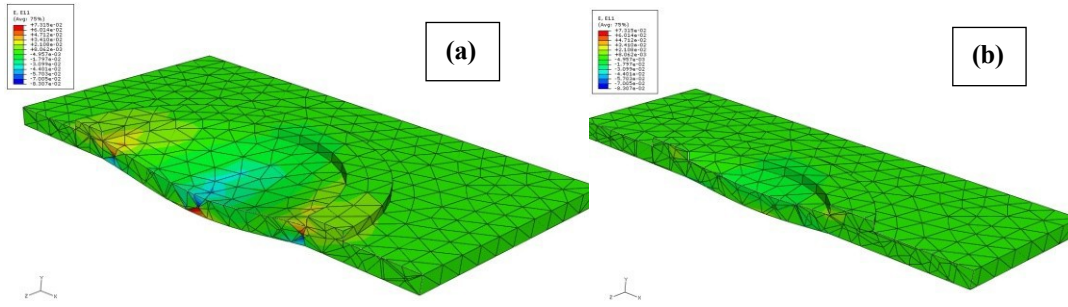


Figure 11. Simulation strain results: (a) in a plan passing through the centre (sensor in diagonal position); (b) in a plan passing parallel to the centre (sensor in vertical position).

According to Figure 12, stress concentrations occur in the region in the circle border and local maximum strain can be found in the centre of the circle. Also, the maximum principal strain presents radial directions from the centre of the circle to the borders, along the longitudinal axis of the fibre.

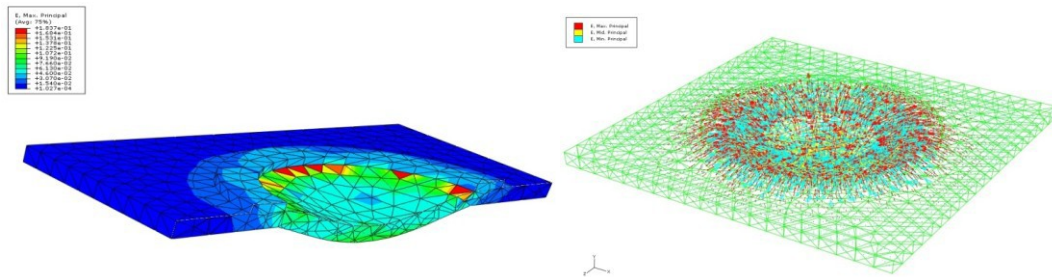


Figure 12. Maximum principal strain for a scale weight prototype made of 10% diluted silicone rubber, with a load of 2500 g (left); Strain principal directions for a scale weight prototype made of 10% diluted silicone rubber, with a load of 2500 g (right).

According to the numerical simulation it is possible to predict that the higher value for this scale weight will be about 1700 g, which corresponds to the strain of break of the FBG sensors (0.4%). In both cases (numerical and experimental; Figure 10) results show a similar linear response. Although this device was only tested up to 0.12% of strain, we may extrapolate from the numerical results that this linear trend is maintained up to the optical fibre strain limit.

## CONCLUSION

This paper reports the first results on the development of a prototype of a weight measuring system using fibre Bragg grating (FBG) sensors embedded in a silicone rubber tray. In summary, it has been shown that both FBG sensors show linear response when embedded in a silicone rubber material and when exposed to weight variations between 0.5g to 500g. Experimental tests enabled to observe the sensors repeatability. A consistent calibration factor of 0.0033 nm/g and a good resolution of 1.69g were obtained. Also, the numerical simulation allowed the verification that the FBG sensors positions are exactly in the regions of higher sensibility to the load. By using a material with lower stiffness the prototype as become more sensible to weight, which could have been otherwise achieved by decreasing thickness or removing some material from the central area of the silicone base, however at the cost of compromising the maximum weight capacity of the prototype.

## ACKNOWLEDGMENTS

The financial support given by the Foundation for Science and Technology (FCT) of Portugal, under project PTDC/EME-PME/108308/2008 (SMARTCOAT), is gratefully acknowledged by the authors.

## REFERENCES

1. A. Vieira, R. de Oliveira, O. Frazão, J. M. Baptista and A. T. Marques, "Effect of the re-coating and the length on fiber Bragg grating sensors embedded in polymer composites", *Materials & Design*, 30(5): 1818-1821, 2009.
2. T. Fresvig, P. Ludvigsen, H. Steen and O. Reikerås, "Fibre optic Bragg grating sensors: An alternative method to strain gauges for measuring deformation in bone", *Medical Engineering & Physics*, 30(1): 104-108, 2008.
3. R. M. Measures, *Structural monitoring with Fiber Optic technology*, Academic Press, London, 2008.
4. C. Frias, O. Frazão, S. Tavares, A. Vieira, A. T. Marques and J. Simões, "Mechanical characterization of bone cement using fiber Bragg grating sensors", *Materials & Design*, 30(5): 1841-1844, 2009.
5. M. Majumder, T. K. Gangopadhyay, A. K. Chakraborty, K. Dasgupta and D. K. Bhattacharya, "Fibre Bragg gratings in structural health monitoring-Present status and applications", *Sensors and Actuators A: Physical*, 147(1): 150-164, 2008.
6. P. Komi, A. Belli, V. Huttunen, R. Bonnefoy, A. Geyssant and J. R. Lacour, "Optic fibre as a transducer of tendomuscular forces", *European Journal of Applied Physiology and Occupational Physiology*, 72(3): 278-280, 1996.
7. C. Frias, H. Faria, O. Frazão, P. Vieira and A. T. Marques, "Manufacturing and testing composite overwrapped pressure vessels with embedded sensors", *Materials & Design*, 31(8): 4016-4022, 2010.
8. M. S. Ferreira, J. Vieira, C. Frias and O. Frazão, "Simultaneous measurement of strain and temperature using fiber Bragg grating sensors embedded in hybrid composite laminates", *Measurement Science and Technology*, 22(4): 045206, 2011.
9. A. W. Morey, G. Meltz and W. Glenn, "Fibre optic Bragg grating sensors", *Fiber Optic and Lasers Sensors VII*, SPIE vol. 1169: 98-107, 1989.